NUMERICAL SIMULATION OF LEAKING HYDROGEN DISPERSION BEHAVIOR

Liang Zhang[1,2], Nan Wang[1,2], XueLun Chang[1,2], JianFu Zhao[3], HuiJie Zhang[4], Hong Chen[4] and FuMing Yang[1,2]
[1] New energy technology research institute, State power investment corporation research institute, South Park, Beijing Future Science city, Beijing 102209, People's Republic of China, 111zhangliang@163.com
[2] Guohe Huaqing (Beijing) Nuclear Power Technology R&D Center, South Park, Beijing Future Science city, Beijing 102209, People's Republic of China
[3] CAS Key Laboratory of Microgravity, Institute of Mechanics, Chinese Academy of Sciences, 15 Beisihuan Xilu, Beijing 100190, People's Republic of China, jfzhao@imech.ac.cn
[4] College of Areospace and Civil Engineering, Harbin Engineering University, Harbin 150001, People's Republic of China, jason@hrbeu.edu.cn

ABSTRACT

As one kind of clean, zero carbon and sustainable energy, hydrogen energy has been regarded as the most potential secondary energy. Recently, hydrogen refueling station gradually becomes one of important distribution infrastructures that provides hydrogen sources for transport vehicles and other distribution devices. However, the highly combustible nature of hydrogen may bring great hazards to environment and human. The safety design of hydrogen usage has been brought to public too. This paper is mainly focused on the hydrogen leakage and dispersion process. A new solver for gaseous buoyancy dispersion process is developed based on OpenFOAM [1]. Thermodynamic and transport properties of gases are updated by library Mutation ++ [2]. For validation, two tests of hydrogen dispersion in partially opened space and closed space are presented. Numerical simulation of hydrogen dispersion behavior in hydrogen refueling station is carried out in this paper as well. From the results, three phases of injection, dispersion and buoyancy can be seen clearly. The profile of hydrogen concentration is tend to be Gaussian in dispersion region. Subsonic H_2 jet in stagnant environment is calculated for refueling station, the relationship between H_2 concentration decay and velocity along the jet trajectory is obtained.

Keywords: hydrogen dispersion, hydrogen refueling station, H_2 concentration decay, OpenFOAM

1.0 INTRODUCTION

As a long-term chemical energy storage form, hydrogen energy is widely promoted. However, the safety assessmentof hydrogen has attracted extensive attention because of the features of hydrogen (0.082 kg/m3 for density, 4~75 vol % for flammability). For a variety of storages and transportation applications, hydrogen will be rapidly diffused due to buoyancy in case of leakage.Besides, hydrogen will be hindered and accumulated in restricted environments when obstacles are in the scene, which greatly increases the possibility of self-ignition. Deflagration and detonation may even occur when the hydrogen concentration meets certain condition. So, investigation of the concentration field and combustible clouds distribution becomes necessary. In order to provide a safety margin, it is important to study the process of hydrogen leakage and dispersion.

For leakage process study, since 1926, it has been found that the tensile strength of steel is greatly reduced by the presence of hydrogen at room temperature [3]. So, great efforts on risk assessment determination have been carried out. Swain M. R. and Swain M.N. [4] discussed a method for hydrogen leak classification in which different type of space for gas injection is considered. Isaac W. E. et al. [5] investigated the hydrogen leaks and deflagration experimentally for indoor use industrial forklifts. However, hydrogen concentrations were derived from O_2 depletion measurements. During

experimental research, risk must be considered. Different facility open end wall arrangements were used to facilitate data acquisition, like in the situation of overpressure. Under the current test conditions, there are still large errors in the measurement of many phenomena, such as the response time of monitoring equipment.

Numerical simulation is an effective method for hydrogen risk assessment. Schefer R.W. et al. [6] developed equations for the calculation of leak flow rates in various leak regimes. Equations are presented for subsonic laminar and turbulent flows, as well as choked (sonic) flow. A chain of models for high pressure unignited H_2-jet from a small leak were developed by Xiao J. [7]. The models are based on isentropic expansion hypothesis and other ideal conditions. Three phases are described in this paper: release of high pressure hydrogen from a reservoir with a small leak; adiabatic expansion to atmospheric pressure; free turbulent H2 mixing into ambient air from the virtual jet origin. Matsuura K. [8] simulated the process of hydrogen dispersion in a partially opened space. The effects of vent position, vent parameter and surrounding atmospheric current on the distribution of hydrogen concentration are shown using steady results by Matsuura K. [8]. Stefano M.D. et al. [9] investigated the hydrogen dispersion in a confined room under non-ventilation, CFD codes is validated by various parameters such as flow and leakage location. Swain M. R. et al. [10] simulated the relative risks for four types of vehicle fuels from which hydrogen is continuously charged into the garage. Distribution of combustible cloud affected by flow rate under venting condition is analyzed.

For hydrogen leakage in hydrogen refueling station, Kim E. et al. [11] studied the hydrogen leak scenario cases with a set of pressure 10~40 MPa and a set of ejecting hole sizes 0.5~1 mm using a commercial CFD tool FLACS. The simulation results are validated with hydrogen jet experimental data and safe distance of fueling facility system is identified. Li J.Y. [12] simulated the leakage and explosion of high pressure hydrogen storage cylinder in the Shanghai World Expo hydrogen refueling station with FLACS. Results showed that the explosion intension and hazard distance are affected by congestion of obstacle region and wind speed. Experiments of high-pressure (40MPa) leak and release into a simulated high-pressure dispending area is carried by Shirvill L.C. et al. [13]. The consequences after explosion is analyzed.

Low pressure hydrogen leak and dispersion in hydrogen refueling station is rarely studied, which may occur on multi-layer packed pipeline or pipeline connection, and this paper is mainly focus on the simulation of this process in stagnant environment. In order to adapt to the full speed range of hydrogen behavior, a new CFD solver is developed based on the frame of OpenFOAM in which thermodynamic and transport properties of gases are obtained by library Mutation ++ [2]. Here, only low pressure hydrogen leak and dispersion is presented and two typical hydrogen dispersion tests are used to validate the code.

2.0 NUMERICAL MODELS

Hydrogen leakage is actually a typical process of convection and dispersion, and the hydrogen leakage from high pressure storage vessel will introduce highly under expanded jet. In the conservative system, compressibility is adopted. In the simulation, the mass fraction transport equation for species H_2, N_2, O_2 is used for analysis,

$$\frac{\partial \rho Y_i}{\partial t} + \nabla \cdot \left(\rho \vec{U} Y_i \right) = \nabla \cdot \left(\nabla \rho D_{i,eff} Y_i \right), \tag{1}$$

Here, Y_i is mass fraction of the ith component. N components are considered in the system, the calculation of the Nth component of inert gas nitrogen in the air is removed. Since the sum of mass ratio must be 1, so the fraction of inert gas can be obtained by $1 - \sum_{i=1}^{i=N-1} Y_i$.

In the term of dispersion, effective dispersion coefficient

$$D_{i,eff} = D_i + D_t,$$

2

Here, D_i is laminar dispersion coefficient, and it should be noted that D_i is corrected by mutation ++ code according to the bulk pressure and temperature. D_t is turbulence dispersion coefficient, for simplicity, $Le = \frac{Sc}{Pr} = 1$ [14] is adopted where $D_t = \alpha_t$ can be obtained.

Here, Le is Lewis number, $Sc = \frac{\mu}{\rho D}$ is Schmidt number, $Pr = \frac{\mu}{\rho \alpha}$ is Prandtl number, α_t is turbulence thermal dispersion.

Energy equation:

The specific enthalpy of mixture is used for energy equation,

$$\frac{\partial \rho h}{\partial t} + \nabla \cdot (\rho \vec{U} h) + \frac{\partial \rho K}{\partial t} + \nabla \cdot (\rho \vec{U} K) - \nabla \cdot (\nabla \alpha_{eff} h) = \frac{\partial p}{\partial t} + \rho \gamma \, , \tag{2}$$

Here, mechanical energy $K = \frac{1}{2} |\vec{U}^2|$, $\gamma = \sum_{i=1}^{i=N} \{ \nabla \cdot \nabla (D_{i,eff} h_i Y_i) \}$ is the transportation of enthalpy due to species dispersion. The effective thermal dispersion coefficient can be obtained by $\alpha_{eff} = \alpha + \alpha_t$, Mutation ++ is used to calculate the laminar thermal dispersion coefficient of mixture α.

Continuity conservation equation:

$$\frac{\partial \rho}{\partial t} + \nabla \cdot (\rho \vec{U}) = 0 \, , \tag{3}$$

Momentum conservation equation:

$$\frac{\partial \rho \vec{U}}{\partial t} + \nabla \cdot (\rho \vec{U} \vec{U}) = -\nabla p + \rho \vec{g} + \nabla \cdot (\mu_{eff} \nabla \vec{U}), \tag{4}$$

The effective kinetic viscosity can be obtained by $\mu_{eff} = \mu + \mu_t$. Here, μ_t is turbulence kinetic viscosity. Mutation ++ is used to calculate the laminar kinetic viscosity of mixture μ.

This new solver is developed based on reactingFoam in the framework of OpenFOAM. A robust algorithm EPPL [15] is used to solve the above equations. Compressible characteristic is considered through ideal gas law, and density ρ is updated after energy equation is solved. Besides, D_i, α, μ, h_i are updated just after energy equation is solved. For validation, two hydrogen dispersion tests in partially opened space and closed space are used for comparison.

3.0 SIMULATIOIN RESULTS

3.1 TEST 1: PARTIALLY OPENED SPACE

For comparison, the first test of hydrogen dispersion in hallway with partially opened space [8] is chosen. Schematic of hallway is given by Fig. 1. In the experiments, gas escapes into unenclosed spaces. In the computational domain, the time series data of hydrogen concentration are sampled at four positions shown in the left of Fig. 1. The right of Fig. 1 shows the experimental model of the hallway, which is made of acrylic acid resin. At both the roof vent and the door vent, the condition of natural ventilation is imposed. Hexahedral mesh structure for the model is used in the setting, k-ε model is adopted for turbulence calculation (as Fig. 2). In the picture, Fig. 2 a) is the mesh for hallway with outside space (17.4×7.442×4.44 m), Fig. 2 b) is the mesh for hallway (2.9×1.22×0.74 m). The total mesh size is 851200. Pure hydrogen leaks into the space with a velocity of 2.03×10^{-2} m/s. The area of the inflow orifice, the roof vent and the door vent are all 0.1524×0.3048 m.
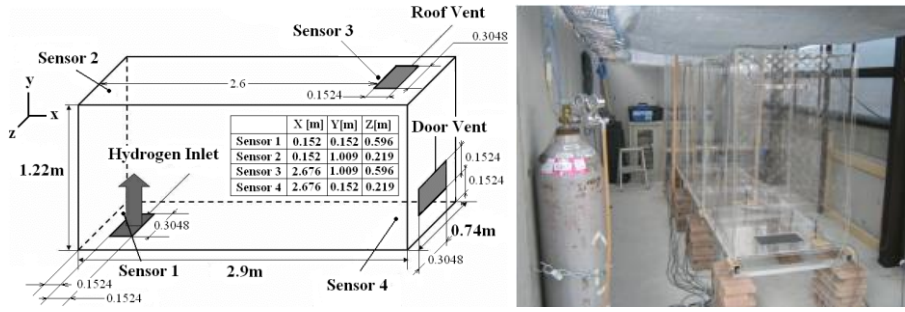
Figure 1. Schematic of hallway [8]
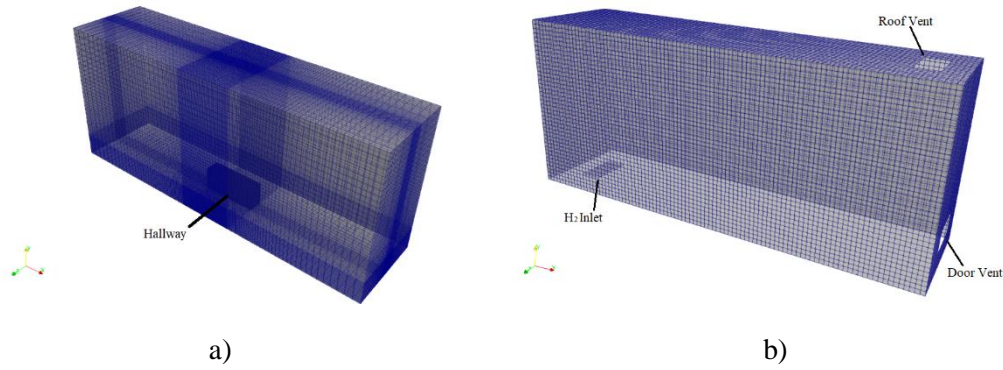

a)   b)

Figure 2. Mesh of hallway with outside space

In Fig. 3, the evolution of hydrogen concentrations are compared with the data provided by paper [8]. The results calculated by our new solver using turbulence model is represented by Fig. 3 a). Experimental data and other calculation results using turbulence model are shown in Fig. 3 b). It can be seen that present CFD results agree well with experimental data and other calculation results. From all the results, it is shown that steady stratification is formed in the end because of turbulence mixing. However, a higher hydrogen concentration for sensor 2 and 3 is obtained during the steady period, it may be caused by the turbulence model chosen in the calculation, and more hydrogen is driven up to the roof.

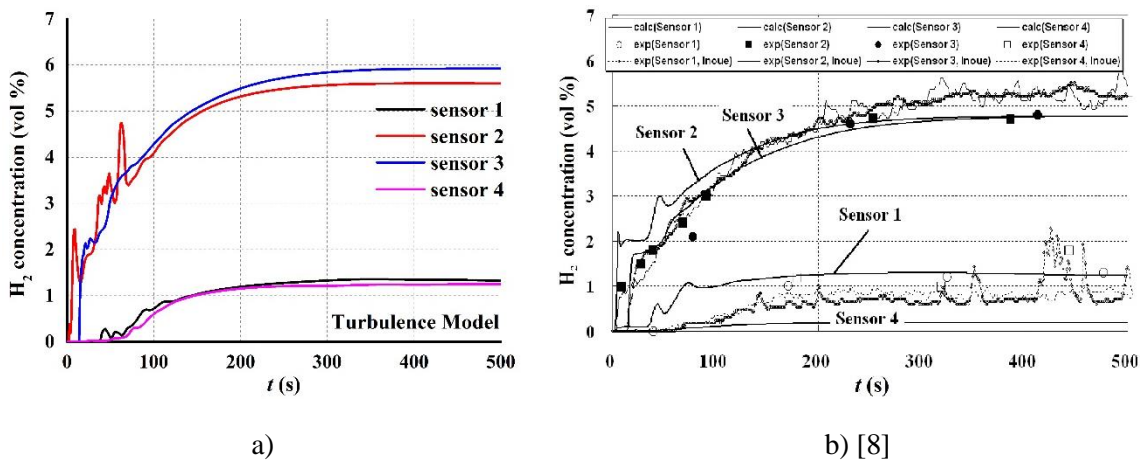a)   b) [8]

Figure 3. Evolution of hydrogen concentration between the computations and the experiments

For the sake of clarity, the evolution of hydrogen concentrations using laminar model are also presented in Fig. 4. Good consistency between the CFD results calculated by our solver and other experiments and simulation results can be obviously seen. So, according to the dimensionless

4

Reynolds number $\text{Re} = \frac{\rho_{H_2} u D}{\mu_{H_2}} \approx 43$ [9], laminar flow may be more suitable for this case. It can be explained that flow regime in the case is mainly under the interaction of dispersion and buoyancy.
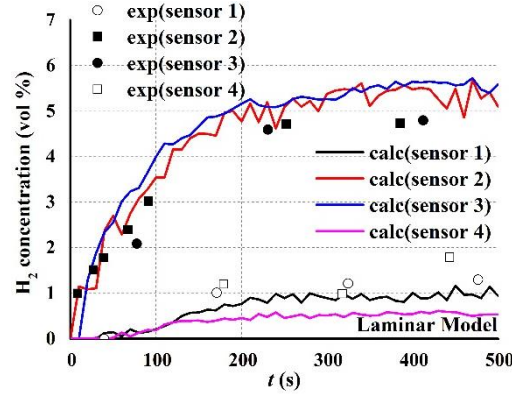

Figure 4. Evolution of hydrogen concentration at sensors using laminar model

3.2 TEST 2: CLOSED SPACE

The second test is hydrogen dispersion in closed space [9] which is 1/15 scaled model for a room of nuclear facility. Hexahedral mesh structure for the model is used in the setting, it is shown in Fig. 5 a). The computational region size is $0.47 \times 0.33 \times 0.20$ m (as Fig. 5 b)). The stationary reference position of $E_{H2}3$ [9] is chosen for the validation. Three types of flow regime and parameters of flow rates [9] is adopted. Besides, inlet orifice diameter is d=0.004 m and the total volume injected is $V = 1.67 \times 10^{-3}$ m^3 for all cases. Injection duration is 1 s, 4 s and 20 s for turbulence model, transition model and laminar model respectively. Four rods, denoted as A, B, C and D in Fig. 5 b) [9], with four sensors on each were set in the enclosure.
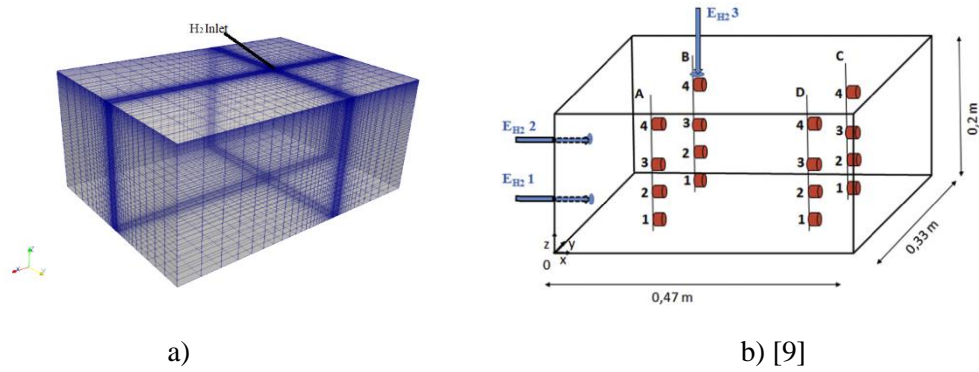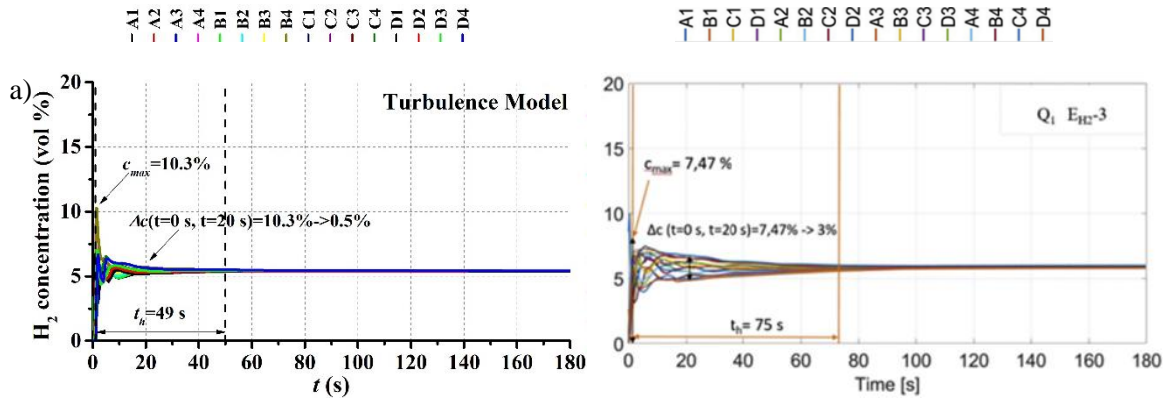

a)

b) [9]

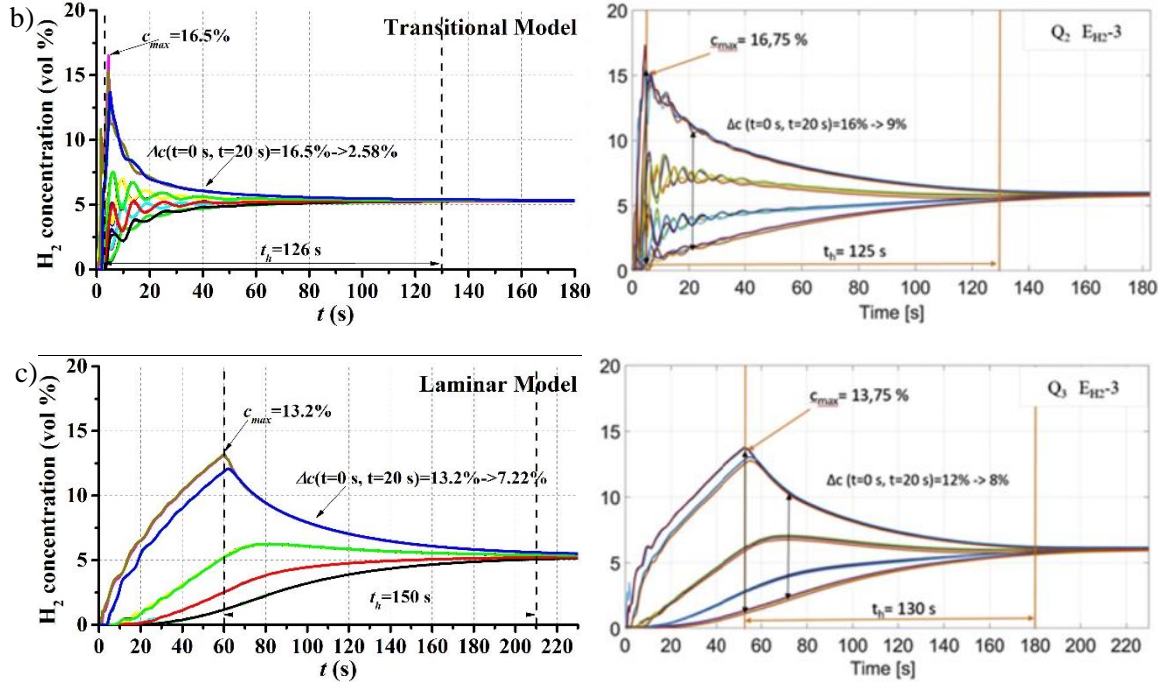Figure 5. Mesh of hallway with outside space

Figure 6. Evolution of hydrogen concentration at sensors using different models

Evolution of hydrogen concentration at sensors is shown in Fig. 6. Left side is the CFD results, right side is experimental results [9]. Three flow models are chosen for comparison: laminar flow, transition flow, turbulence flow. What needs to be clarified is that the peak concentration is around 10 vol % too showed in the right of the picture Fig. 6 a). It's not clear why 7.47% is written by the authors. So, it can be seen that all the maximum hydrogen concentrations agree well with the experimental data, except that a lag occurs in the case of the laminar flow. During the experiment [9], the mass injection is controlled to be slow in the case of low flow rate, which leads to the actual injection time is less than expected. To ensure the total injection volume, injection time 60 s is changed for the simulation. The concentration variation Δc at $t=0$, 20 s after the end of injection is also described in the picture. From the results, some deviations is obtained in the hydrogen dispersion process, which may be caused by the selection of turbulence model. In this paper, the RAS k-ε model shown in Table 1 is adopted which may cause extensive mixing.

Table 1. Turbulence model setup.

parameter	Turbulence flow	Transition flow	Laminar flow
k	80.43	7.125	-
ε	29630	781	-
Re	4975	1245	85

3.3   TEST 3: HYDROGEN REFUELING STATION

The third test is hydrogen dispersion in hydrogen refueling station. The layout of refuelling station is shown in Fig. 7. It is a full scale model with size of $20 \times 25 \times 5.3$ m. SnappyHexMesh method is used for creating the mesh of fluid region, especially the downwind region of the orifice (as Fig. 7 b)), total mesh of 937396 cells is generated (maximum cell volume: 2.21×10^{-2} m³, minimum cell volume 9.77×10^{-9} m³). To analyse the hydrogen dispersion, a circular break with radius 0.02 m in the surface centre of leak tank is postulated (as Fig. 7 b)) which is equivalently considered as a break at the pipe joint. The aim of the present study is not the sonic flow, but rather the special leak for the far field away from the orifice. From another point of view, according to the data [7], the velocity decelerates rapidly along the jet trajectory, so the leak velocity of 200 m/s is reasonable for the case.
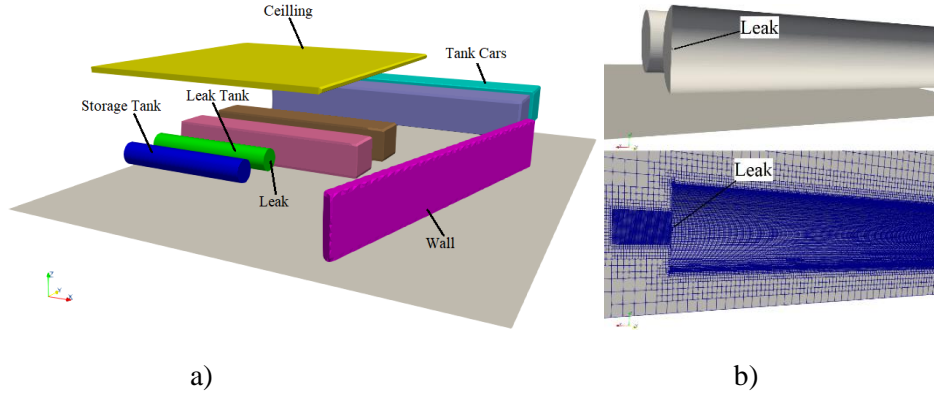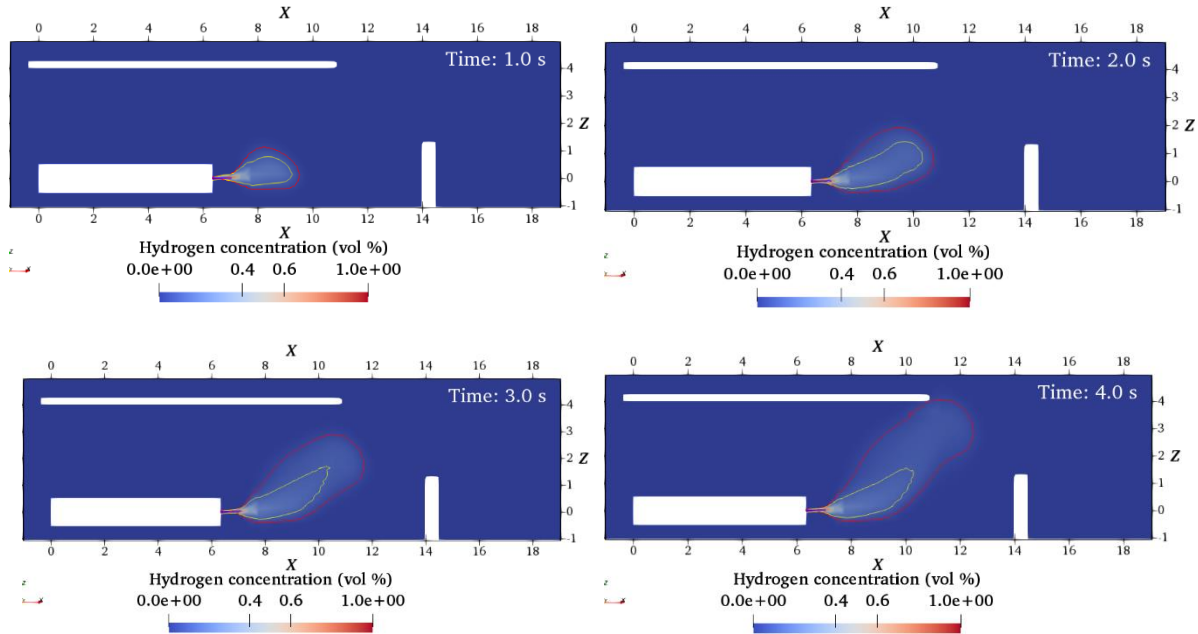
Figure 7 Structure of hydrogen refueling station

Evolution of hydrogen concentration in hydrogen refueling station is shown in Fig. 8. Three hydrogen contours (4, 10, 75 vol %) are displayed in the plane sliced along the tank axis. The lower flammable concentration 4 vol %, stable turbulent diffusion flame region of hydrogen concentration 10 vol % and upper flammable concentration 75 vol % are distributed from inside to outside. Three phases can be seen clearly in the results, injection, dispersion and buoyancy. Due to high flow rate, the region of inertial force dominated is extended 0.64~0.67 m during the dispersion with less disturb. After that, hydrogen is spread because of molecular dispersion, the distribution of H_2 in radial directions is approximately the same. Finally, buoyancy plays an important role in the far field because of relative high H_2 concentration. The max radial spread distance along the trajectory is about 2.68 m and spread distance in x-axis is up to 2.87 m for 4 vol % when $t = 6.0$ s, and the distances are within the sense range of single sensor. In these pictures, upper concentration 75 vol % is only limited near the orifice. Above all, high risk can be evaluated for the case without any natural or mechanical ventilation, sensors should be placed along the jet trajectory which makes sure fast response.
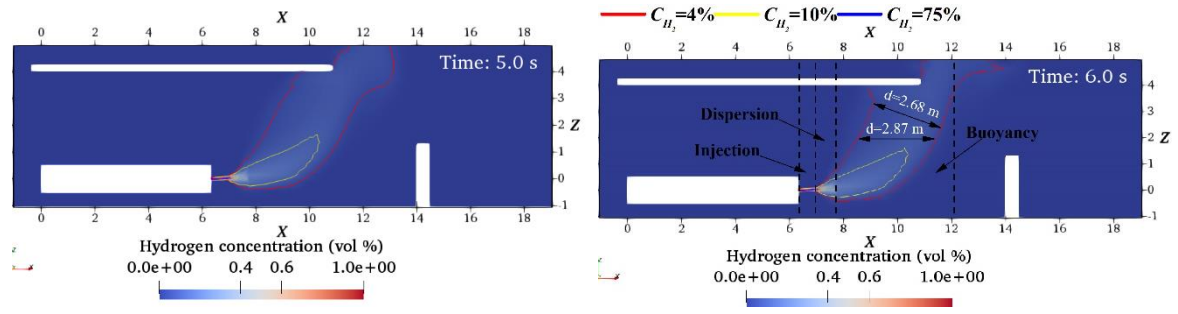
Figure 8 Evolution of hydrogen concentration in hydrogen refueling station

Evolution of three hydrogen contours (4, 10 and 75 vol %) in seven slices is displayed in Fig. 9. The slices are scattered with equal distance of 1 m. To capture the main features, the first slice is 0.65 m away from the gas outlet. Hydrogen radial dispersion is shown in these pictures. Due to the low density of hydrogen, no obvious backflow can be seen when hydrogen touches the ceiling wall. Besides, phase of dispersion can also be seen in the second slice which is similar to the Gaussian distribution.
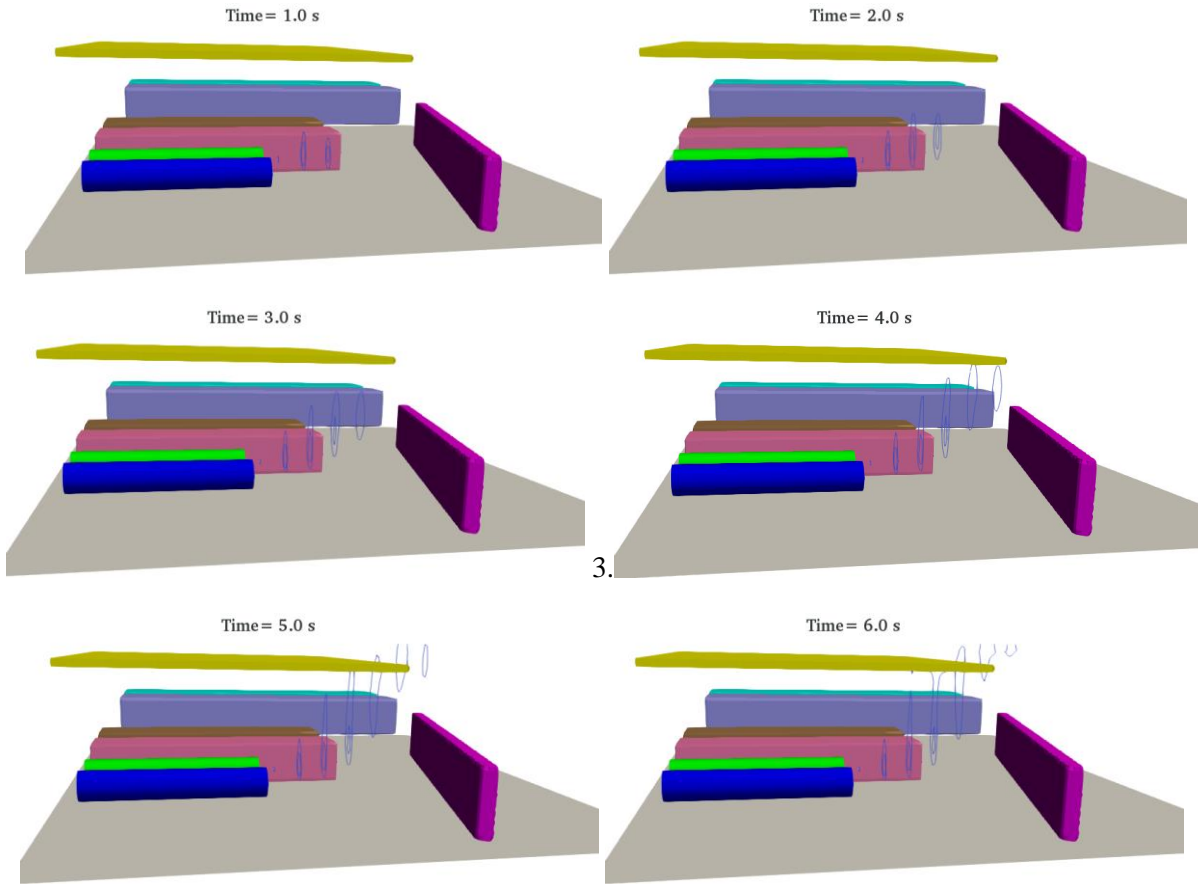

Figure 9 Evolution of hydrogen concentration in hydrogen refueling station (radial slice)

Evolution of hydrogen concentration along the axial direction is shown in Fig. 10. From the results, a sharp reverse change exists in the flow direction due to the air entrainment into the jet. However, there is no regularity. The starting point of reverse change is 0.64~0.8 m away from the orifice which is just in the second phase.
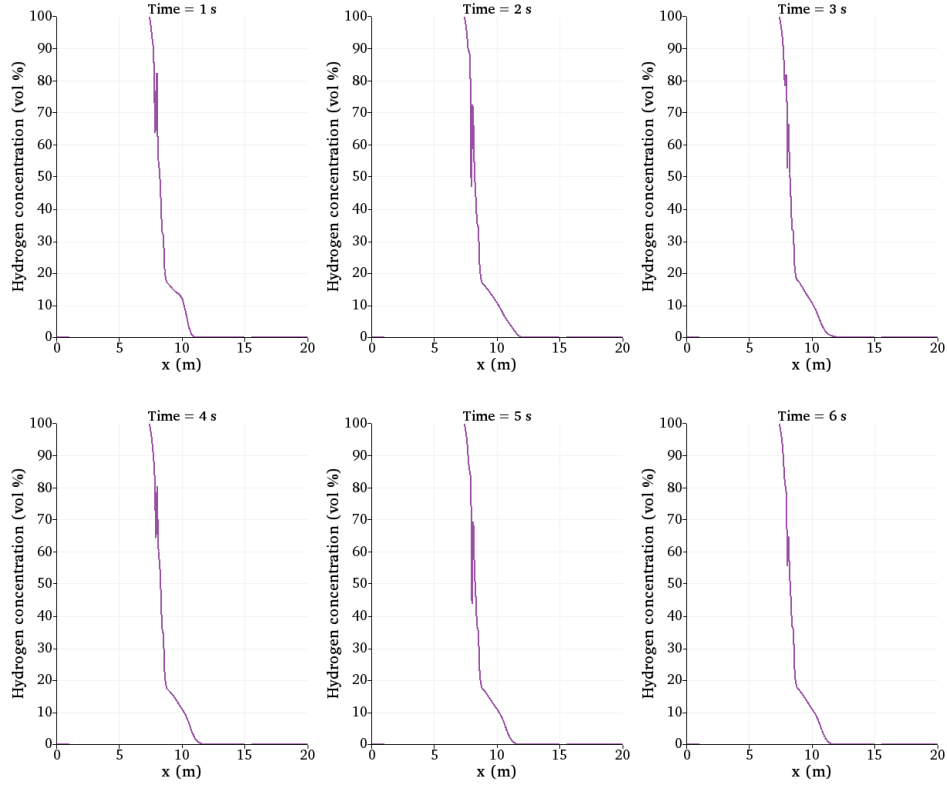
8

Figure 10 Evolution of hydrogen concentration along the axial direction

Inspite of consideration of various external factors, many ideal conditions are assumed by theoretical methods. To make the achievements more close to practical application, stagnant environment is adopted in the paper. For the first time, the relationship between hydrogen concentration and jet velocity is introduced to characterize H_2 concentration decay along the trajectory. Equation (5) given by Xiao et al. [7] is used for subsonic incompressible turbulence free jets, and H_2 concentration decay is found to follow the hyperbolic law along the jet centerline.

$$C_{sH_2} = K \frac{D_{eq}}{S+S_0},$$
(5)

Here, K is the slope, S is distance from the nozzle along the trajectory, S_0 is the integral model's virtual origin displacement, $D_{eq} = D_0 \left(\frac{\rho_r}{\rho_a}\right)^{0.5}$ is the normalized diameter, the density of the ambient atmosphere is ρ_a, the density of reservoir is ρ_r. According to the integral model, $S_0 = 30D_0$ is used in sonic flow. D_0 is the orifice diameter. In this case, no lower flammability limit region is obtained along the jet trajectory which can also be seen in Fig. 8.

In Fig. 11, H_2 concentration along the trajectory is given by two representations. In the left picture, four test cases [7] of sonic flow with the upstream mass flow rate of 3.3 g/s from orifices with diameters of 1 mm and 2 mm are chosen for comparison. Although the experimental conditions are distinct between the tests [7] and the case carried in this paper, obviously different distribution of H_2 concentration can be seen. In the left picture, experimental data is presented with "case*_exp", results calculated by integral model is companied with "case*_int" and results calculated by the new solver is "calc". H_2 concentration decays for the four test cases obey the law $C_{sH_2} \approx 37.6 \frac{D_{eq}}{S+S_0}$. While three phases occur along jet trajectory, and K equals to 1000, 33.3, 111.1 respectively. In the right figure, the relationship $U_s \sim \frac{S+S_0}{D_{eq}}$ is obtained by fitting experimental data, and H_2 concentration decay is derived by U_s for stagnant case 1. From the results, $C_{H_2} \approx \frac{1.02}{20/U_s^{1.27}+1}$ can be obtained. Slowly H_2

concentration decay exists in the region of inertial force dominated, after that, similar hyperbolic law happens along the jet centreline.
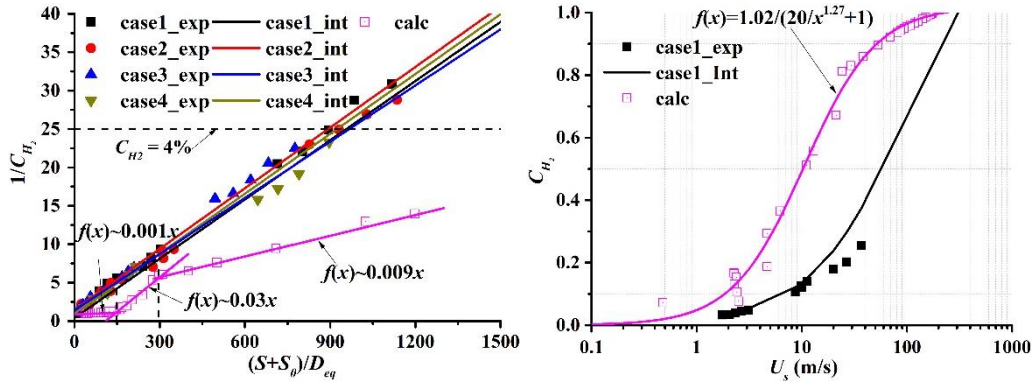

Figure 11 H_2 concentration along the jet trajectory

CONCLUSIONS

In this paper, a new solver based on OpenFOAM [1] for gaseous buoyancy dispersion process is developed. Thermodynamic and transport properties of gases are obtained by library Mutation ++ [2]. Two hydrogen dispersion tests are used for comparison. Good agreement is obtained for all the test, adequate turbulence model should be chosen for high flow rate cases. From the results, this solver can be used to predict the process of hydrogen dispersion and buoyant.

Evolution of hydrogen concentration without ignition in stagnant environment for hydrogen refueling station is analysed in this paper. Three phases can be seen clearly during the process of leakage. Under given conditions, the max radial spread distance is 2.68 m and max x direction spread is 2.87 m for 4 vol % when time = 6.0 s. Upper concentration 75 vol % is only limited near the orifice. Hydrogen distribution is similar to the Gaussian distribution in dispersion phase. A sharp reverse change exists in the flow direction due to the air entrainment into the jet in the second phase. High risk can be evaluated for the case. Four experimental tests are used to show the difference of H_2 concentration decay between upstream leak and horizontal jet leak. For horizontal jet leak, slowly H_2 concentration decay exists in the region of inertial force dominated, similar hyperbolic law happens along the jet centreline for both leak cases.

To valuate specific risk assessment, natural or mechanical ventilation will be considered in future study. High pressure will also be the key point of research.

ACKNOWLEDGMENTS

REFERENCES

1. OpenFOAM. The Open Source CFD Toolbox, User Guide. 2013. Available online: https://cfd.direct/openfoam/user-guide/ (accessed on 24 Febuary 2017).
2. B. and Magin T.E., "Development of Mutation++: Multicomponent Thermodynamic and Transport Properties for Ionized Plasmas written in C++," 11th AIAA/ASME Joint Thermophysics and Heat Transfer Conference, AIAA Paper 2014-2966.
3. Pfeil L.B., M. Sc. and A.R.S.M., The effect of occluded hydrogen on the tensile strength of iron. *Proc. R. Soc. Lond. A*, Vol 112, Pl. 6, 1926, pp. 182-195.

4. Swain M.R. and Swain M.N., Passive Ventilation Systems for The Safe Use of Hydrogen. *International Journal of Hydrogen Energy*, **21**, No. 10, 1996, pp. 823–835.

5. Isaac W.E., William G.H., Greg H.E., Erik G.M. and Mark A.G., Experimental investigation of hydrogen release and ignition from fuel cell powered forklifts in enclosed spaces. *International Journal of Hydrogen Energy*, 37, 2012, pp. 17446-17456.

6. Schefer R.W., Houf W.G., San Marchi C., Chernicoff W.P. and Englom L., Characterization of Leaks from Compressed Hydrogen Dispensing Systems and Related Components. International *Journal of Hydrogen Energy*, 31, 2006, pp. 1247-1260.

7. Xiao J., Travis J.R. and Breitung W., Hydrogen Release from A High Pressure Gaseous Hydrogen Reservoir in Case of A Small Leak. *International Journal of Hydrogen Energy*, 36, 2011, pp. 2545-2554.

8. Matsuura K., Kanayama H. and Tsukikawa H., Numerical simulation of leaking hydrogen dispersion behavior in a partially open space. *International Journal of Hydrogen Energy*, 33, No. 1, 2008, pp. 240-247.

9. Stefano M.D., Rocourt X. Sochet I. and Daudey N., Hydrogen Dispersion in A Closed Environment. *International Journal of Hydrogen Energy*, 2018, pp. 1-10.

10. Swain M.R., Shriber J. and Swain M.N., Comparisons of Hydrogen, Natural Gas, Liquified Petroleum Gas, and Gasoline Leakage in A Residential Garage. *Energy Fuels*, No. 12, 1998, pp. 83-89.

11. Kim E., Park J., Cho J.H. and Moon I. Simulation of Hydrogen Leak and Explosion for The Safety Design of Hydrogen Fueling Station in Korea. *International Journal of Hydrogen Energy*, 38, 2013, pp. 1737-1743.

12. Li J.Y., Zhao Y.Z. and Zheng J.Y. Simulation and Analysis on Leakage and Explosion of High Pressure Hydrogen in Hydrogen Refueling Station. *Journal of Zhejiang University (Engineering Science Edition)*, 49(7), 2015, pp, 1389-1394.

13. Shirvill L.C., Roberts T.A., Royle M., Willoughby D.B. and Gautier T. Safety Studies on High-pressure Hydrogen Vehicle Refueling Stations: Releases into A Simulated High-pressure Dispensing Area. *International Journal of Hydrogen Energy*, 37, 2012, pp. 6949-6964.

14. Haβlberger J., Numerical Simulation of Deflagration to Detonation Transition on Industry Scale. PhD. Thesis, 2017.

15. Zhang H.J., Zhu W.B. and Chen H., A robust and efficient segregated algorithm for fluid flow: The EPPL method. *Journal of Computational Physics*, 2020, Vol. 423, pp. 109823 1-18.